C–H Activation

DOI: 10.1002/anie.201203163

Intramolecular C–H Bond Activation through a Flexible Ester Linkage**

Christopher J. Shaffer, Detlef Schröder, Christoph Gütz, and Arne Lützen**

Dedicated to Professor François Diederich on the occasion of his 60th birthday

The selective functionalization of alkanes is a hallmark challenge within transition-metal catalysis. This important field continues to be advanced by fundamental investigations of ion/molecule reactions in the gas phase.[1] Conceptually, diatomic metal-oxide ions (e.g., MgO^+, VO^+, FeO^+, NiO^+, and PtO^+) have provided many of the most impressive results in this field and have even demonstrated remarkable reactivity with methane;[2] recently, also the reactive CuO^+ cation has been studied.[3]

The strength of these ions as functional oxidants, however, is often in contrast to their moderate selectivity in reactions with more complex substrates.[4] In an effort to improve selectivity through the application of adaptable ligands, we have studied the reaction of phenanthroline-ligated CuO^+ with propane.[5] Despite the improvement brought by ligation, the selectivity could not be improved past an effective 1:5 preference for the activation of primary versus secondary C–H bonds.

In an effort to increase the regiocontrol and to provide perspectives for a possible transfer to the condensed phase, we have looked towards synthetic advances in regioselective C–H functionalization. Specifically, chemists have long used the distance limitations inherent in intramolecular reactions to control the regioselectivity of C–H functionalization reactions.[6–9] Unfortunately, these concepts are also limited by weak activation interactions[6] or are dependent on irregular directing-group effects within the carbon framework.[7a]

Herein we offer a means of intramolecular regioselective control in C–H bond activation combined with the potency and catalytic turnover delivered from transition-metal catalysis. To this end, a bipyridine unit as a tunable ligand is coupled with a long-chain alkyl group through an ester linkage. Synthetically, 2,2′-bipyridine-5-carboxylic acid (**1**)[10] is easily converted into the ester **2** (Scheme 1).

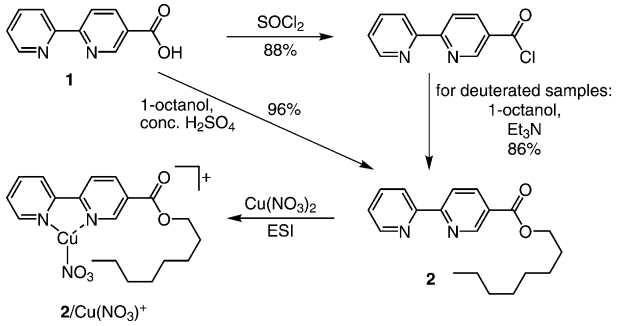

Scheme 1. Synthesis of **2** and electrospray ionization to generate **2**/$Cu(NO_3)^+$.

Electrospray ionization (ESI) of a solution of **2** in methanol/water (1:1) containing an equimolar amount of copper nitrate generates the ion **2**/$Cu(NO_3)^+$ in large abundance.[11–15] Collision-induced dissociation (CID) of mass-selected ions is used to monitor the fragmentation processes and the reactions preceding fragmentation. The major ionic product upon CID of **2**/$Cu(NO_3)^+$ (*m*/*z* 437) corresponds to **1**/$Cu(NO_3)^+$ (*m*/*z* 325) which arises by ester cleavage concomitant with elimination of octene. Competitive with the ester fragmentation are losses of $NO_2^{\bullet}$ and $NO_3^{\bullet}$, respectively. While the latter process leads to the copper(I) complex **2**/Cu^+ (*m*/*z* 375), the loss of $NO_2^{\bullet}$ leads to an ion $\mathbf{X}^+$ with *m*/*z* 391. By monitoring the appearance of these ions upon CID we observed that although ester cleavage is favored, $NO_2^{\bullet}$ and $NO_3^{\bullet}$ losses occur at similar threshold collisional energies (Figure S1 in the Supporting Information).

Upon CID of mass-selected $\mathbf{X}^+$, two major fragments were observed, both occurring at higher collisional energies than that required for the fragmentation of **2**/$Cu(NO_3)^+$. Much like in **2**/$Cu(NO_3)^+$, the predominant dissociation pathway leads to the ester-cleavage product **1**/Cu^+ (*m*/*z* 263). However, the loss of water to produce $[\mathbf{X}-H_2O]^+$ (*m*/*z* 373) competes to a significant extent (Figure 1). The occurrence of dehydration suggests that, at some point, ion $\mathbf{X}^+$ or a transient ion of the same mass can promote an activation of C–H bonds in ligand **2**. A plausible suggestion is that the loss of $NO_2^{\bullet}$ from **2**/$Cu(NO_3)^+$ leads to the copper–oxo species **2**/CuO^+ (*m*/*z* 391) with a formal Cu^{III} center. The reactive metal-oxide cation may then activate a C–H bond of the alkyl chain, followed by reductive elimination[16] to afford Cu^I complexes of the corresponding alcohols, for example, the regioisomers **3**/Cu^+, **4**/Cu^+, and **5**/Cu^+ (Scheme 2, all also

[*] Dr. C. J. Shaffer, Dr. D. Schröder
Institute of Organic Chemistry and Biochemistry
Academy of Sciences of the Czech Republic
Flemingovo náměstí 2, 16610 Prague 6 (Czech Republic)
E-mail: schroeder@uochb.cas.cz
C. Gütz, Prof. Dr. A. Lützen
Kekulé-Institute of Organic Chemistry and Biochemistry
University of Bonn
Gerhard-Domagk-Strasse 1, 53121 Bonn (Germany)
E-mail: arne.luetzen@uni-bonn.de

[**] This work was supported by the Academy of Sciences of the Czech Republish (RVO 61388963) and the European Research Council (AdG HORIZOMS).

Supporting information for this article is available on the WWW under http://dx.doi.org/10.1002/anie.201203163.

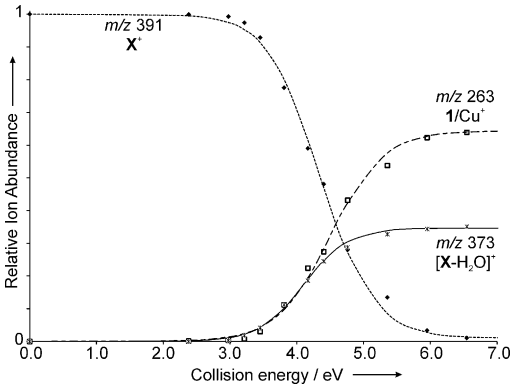

Figure 1. Plot of the energy-dependent CID of $\mathbf{X}^+$ showing the competition of ester cleavage to yield $\mathbf{1}/Cu^+$ and with neutral octene as well as dehydration to afford the ion $[\mathbf{X}-H_2O]^+$.

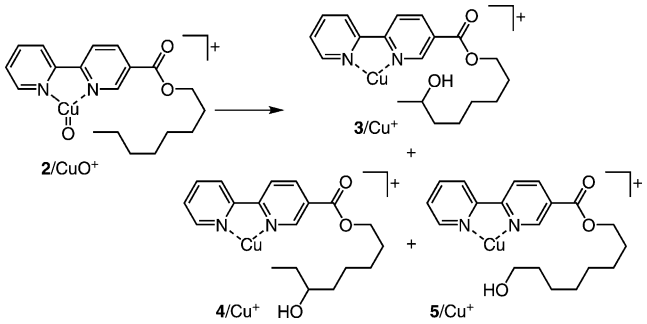

Scheme 2. Oxygen insertion into a C–H bond of $\mathbf{2}/CuO^+$ to yield the complexes of the corresponding alcohols **3**–**5**.

m/*z* 391), from which water elimination to the corresponding olefin complexes can proceed.

Solely reliant on ion masses and collision energies, this experiment is not able to distinguish whether the insertion process occurs with the formation of $\mathbf{X}^+$ or is concurrent with elimination and formation of $[\mathbf{X}-H_2O]^+$. Moreover, the mass spectrometric data does not allow the direct determination of the site of C–H bond activation, because a measurable mass difference occurs only after the elimination has taken place; for example, we cannot distinguish between insertion of oxygen in an ω-C–H bond followed by 1,2-dehydration and (ω-1)-C–H bond activation with subsequent loss of water.

In order to determine the origin of the hydrogen atoms involved in the loss of water from $\mathbf{X}^+$, we investigated isotopologues of **2** with deuterated aliphatic chains. At first, exclusive loss of D_2O upon perdeuteration of the octyl group ($[D_{17}]$-$\mathbf{X}^+$) confirms the ester moiety as the source of the hydrogen atoms involved in water formation and not the 2,2′-biypyridine moiety (Figure 2a).

Deuterium labeling at the terminal position in $[8,8,8\text{-}D_3]$-$\mathbf{X}^+$ results in an approximate 1:1 ratio of H_2O and HDO losses. The substantial amount of HDO loss reveals oxidation at the terminus of the alkyl chain. Deuteration of the adjacent position in $[7,7\text{-}D_2]$-$\mathbf{X}^+$ leads to a 1:5 ratio of H_2O and HDO loss, suggesting a high selectivity for C–H bond activation at the three most terminal carbon atoms. Based on the the kinetic isotope effect of $k_H/k_D = 1.4$ found for C–H bond

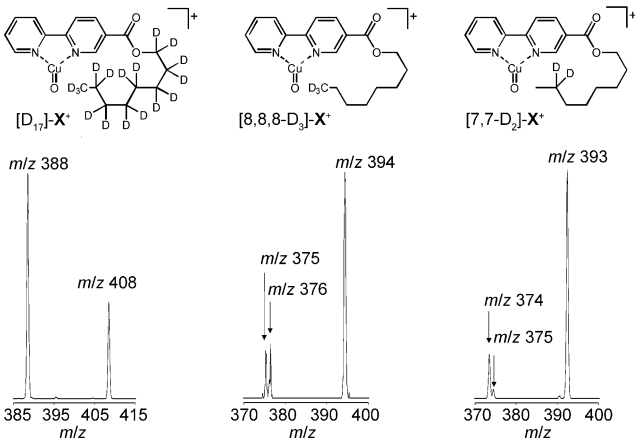

Figure 2. Region of the parent ion and the dehydration product upon CID of the deuterium-labeled species $[D_{17}]$-$\mathbf{X}^+$, $[8,8,8\text{-}D_3]$-$\mathbf{X}^+$, and $[7,7\text{-}D_2]$-$\mathbf{X}^+$.

activation of propane by (phenanthroline)CuO^+ [5] the ratios shown in Figure 2 imply a selectivity of 58% for dehydrogenation across C(7)/C(8), 30% for dehydrogenation across C(6)/C(7), and 12% for more internal positions. This selectivity is significant as there is no directing effect other than the distance from the ester linkage.

Ion-mobility mass spectrometry (IMMS) provides a unique opportunity to investigate structural effects in gas-phase ions.[17] In addition to conventional MS, IMMS separates ions not just by mass, but also by shape.[18] Accordingly, we extended the above studies with IMMS investigations of the ions generated by ESI.[19,20]

For similar types of ions, plotting their arrival times (t_a) versus *m*/*z* in most instances leads to linear correlations, as found for the ions $\mathbf{1}/Cu(NO_3)^+$ (*m*/*z* 325), $\mathbf{2}/Cu^+$ (*m*/*z* 375), and $\mathbf{2}/Cu(NO_3)^+$ (*m*/*z* 437). However, the arrival times for ions $\mathbf{X}^+$ and $[\mathbf{X}-H_2O]^+$ with *m*/*z* 391 and 373, respectively, are significantly shorter than expected from this correlation (Figure 3). The greater mobilities of these ions can be

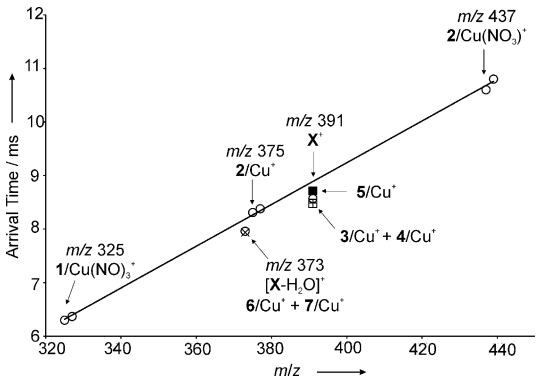

Figure 3. Measured arrival times (t_a in ms) of various mass-selected ions generated by ESI of dilute solutions of $Cu(NO_3)_2$ in methanol/water with either ligand **2** (marked as ○) or the authentic alcohol regioisomers **3**–**5** (marked as +, □, and ■, respectively) or the corresponding olefins **6** and **7** (both marked as ×) as a function of the mass-to-charge ratio; at *m*/*z* 373, the × und ○ symbols overlap. In some cases, the corresponding ^{63}Cu and ^{65}Cu isotopes are both plotted to demonstrate the linearity of mass effects.

rationalized by assuming a recoil of the functionalized alkyl chain to the copper center, such that the shapes of these species become more compact. Interestingly, the shorter arrival time of $\mathbf{X}^+$ suggests that Cu coordination occurs in this ion as well. As it is unlikely that a purely aliphatic chain coordinates with copper, we hypothesized that we already observe a C–H-activated product, rather than **2**/CuO^+. Accordingly, we synthesized the authentic ligand components for each of the proposed oxidation products, that is, ligands **3**–**5**. Next, each of these ligands was measured separately in a solution of $Cu(NO_3)_2$ with an excess of $NH_2OH{\cdot}HCl$ to encourage the formation of the corresponding Cu^I complexes **3**/Cu^+, **4**/Cu^+, and **5**/Cu^+, (all m/z 391). The resulting ions show subtle variations in arrival times, but cumulatively overlay the broad arrival time observed for $\mathbf{X}^+$, which we hence assign to a mixture of these hydroxylation products. This assignment is further supported by B3LYP/6-311 + G(2d,p) calculations,[21] which predict the singlet states of the C–H-insertion products **3**/Cu^+, **4**/Cu^+, and **5**/Cu^+ to be 61, 64, and 59 kcal mol^{-1}, respectively, lower in energy than the triplet state of **2**/CuO^+. Based on the computed geometries, the cross sections of **3**/Cu^+, **4**/Cu^+, and **5**/Cu^+ are estimated as 161, 160, and 158 Å^2, respectively, compared to a value of 187 Å^2 for **2**/CuO^+.[22] The significantly larger cross section of **2**/CuO^+ rules out that this structure would correspond to $\mathbf{X}^+$. These results imply that C–H bond activation is facile and occurs already with the loss of $NO_2^{\bullet}$ and not only during CID of m/z 391.[23] Hence, it appears that $NO_2^{\bullet}$ loss from **2**/$Cu(NO_3)^+$ leads to the high-valent copper–oxo species **2**/CuO^+ only as a transient species and is then followed by intramolecular C–H bond activation to form the corresponding Cu^I complexes **3**/Cu^+, **4**/Cu^+, and **5**/Cu^+, respectively.

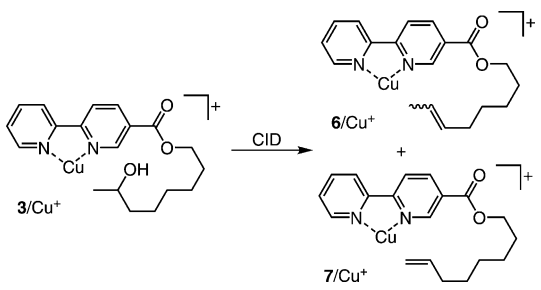

Scheme 3. Dehydration of **3**/Cu^+ to create the regioisomers **6**/Cu^+ and **7**/Cu^+; note that water elimination from **4**/Cu^+ might also lead to **6**/Cu^+ and loss of H_2O from **5**/Cu^+ gives rise to **7**/Cu^+, respectively.

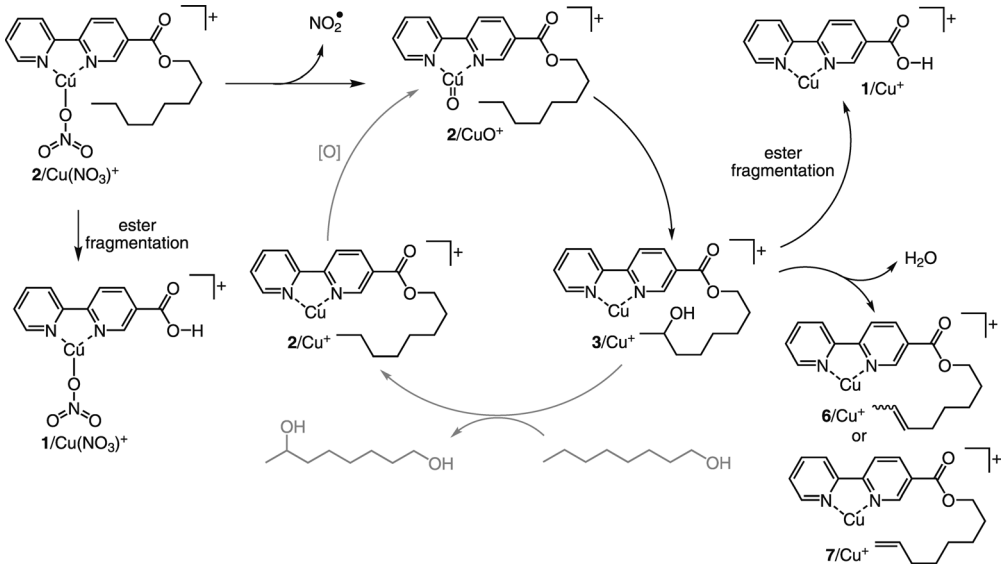

Scheme 4. Gas-phase reactivity and theoretical completion of catalytic cycle.

As mentioned above, also the small t_a value of the ion with m/z 373 implies a difference in shape, which is ascribed to a coordination of copper to the olefinic moiety in the side chains of **6**/Cu^+ and **7**/Cu^+, respectively (Scheme 3). This speculation is confirmed by Cu^+ complexes of authentic samples of **6** and **7**, whose arrival times match that of the $[\mathbf{X}-H_2O]^+$ ion generated from **2**/$Cu(NO_3)^+$.

In summary, our experiments suggest the following sequence of events (Scheme 4). Initial homolysis of the N–O bond in **2**/$Cu(NO_3)^+$ leads to the high-valent copper–oxo species **2**/CuO^+, which then rapidly undergoes C–H bond activation to give the corresponding alcohol complexes **3**/Cu^+, **4**/Cu^+, and **5**/Cu^+, respectively (only the former is shown in Scheme 4). Transesterification with excess alcohol in solution should make it possible for the tethered alcohol to be replaced by a fresh reductant leading to **2**/Cu^+, from which re-oxidation closes the catalytic cycle. The ester fragmentation observed in the mass spectrometric experiments, therefore, is not a detriment, because in order for this proof of concept to be effective in solution, ester exchange must be competitive with oxidation. In this context, we note that after a day of storage, the solutions of **2** and $Cu(NO_3)_2$ in methanol/water show degradation to the corresponding methyl esters, thereby demonstrating the facile occurrence of transesterification in solution.

In the present gas-phase experiments, we are not able to close the catalytic cycle.[24] However, re-oxidation of the copper species and ester exchange are feasible concepts since it is now established that intramolecular C–H bond activation can occur. This gives additional credence to our proposal that similar reactivity can be identified in solution in which that the oxidant can be tuned appropriately to create reactive metal–oxo species under ambient conditions.

Received: April 24, 2012
Published online: July 2, 2012

Keywords: C–H activation · copper · gas phase · ion mobility · oxidation

[1] J. Roithová, D. Schröder, *Chem. Rev.* **2010**, *110*, 1170 – 1211.
[2] H. Schwarz, *Angew. Chem.* **2011**, *123*, 10276 – 10297; *Angew. Chem. Int. Ed.* **2011**, *50*, 10096 – 10115.
[3] N. Dietl, C. van der Linde, M. Schlangen, M. K. Beyer, H. Schwarz, *Angew. Chem.* **2011**, *123*, 5068 – 5072; *Angew. Chem. Int. Ed.* **2011**, *50*, 4966 – 4969.
[4] The dixoide cations CrO_2^+ and PtO_2^+, for example, are among the most reactive metal-oxide cations in the gas phase, but they already show low selectivity in product formation even with methane as the most simple hydrocarbon substrate, see: a) A. Fiedler, I. Kretzschmar, D. Schröder, H. Schwarz, *J. Am. Chem. Soc.* **1996**, *118*, 9941 – 9952; b) M. Brönstrup, D. Schröder, I. Kretzschmar, H. Schwarz, J. N. Harvey, *J. Am. Chem. Soc.* **2001**, *123*, 142 – 147.
[5] D. Schröder, M. C. Holthausen, H. Schwarz, *J. Phys. Chem. B* **2004**, *108*, 14407 – 14416.
[6] R. Breslow, S. Baldwin, T. Flechtner, P. Kalicky, S. Liu, W. Washburn, *J. Am. Chem. Soc.* **1973**, *95*, 3251 – 3262.
[7] a) D. Yang, M.-K. Wong, X.-C. Wang, Y.-C. Tang, *J. Am. Chem. Soc.* **1998**, *120*, 6611 – 6612; b) S. Das, G. W. Brudvig, R. H. Crabtree, *J. Am. Chem. Soc.* **2008**, *130*, 1628 – 1637.
[8] For gas-phase variants of remote functionalization, see: H. Schwarz, *Acc. Chem. Res.* **1989**, *22*, 282 – 287.
[9] For remote functionalization of carbonyl compounds in the gas phase, see: a) G. Czekay, K. Eller, D. Schröder, H. Schwarz, *Angew. Chem.* **1989**, *101*, 1306 – 1308; *Angew. Chem. Int. Ed. Engl.* **1989**, *28*, 1277 – 1278; b) D. Schröder, H. Schwarz, *J. Am. Chem. Soc.* **1990**, *112*, 5947 – 5953; c) D. Schröder, H. Schwarz, *J. Am. Chem. Soc.* **1993**, *115*, 8818 – 8820; d) D. Schröder, W. Zummack, H. Schwarz, *J. Am. Chem. Soc.* **1994**, 116, 5857 – 5864.
[10] U. Kiehne, A. Lützen, *Org. Lett.* **2007**, *9*, 5333 – 5336.
[11] The experiments were performed using a Finnigan LCQ Classic ion-trap mass spectrometer[12] which bears a conventional ESI source consisting of the spray unit (typical flow rates ranged between 5 and 30 $\mu L\,min^{-1}$; typical spray voltage was 5 kV) with nitrogen as a sheath gas, followed by a heated transfer capillary (kept at 200 °C), a first set of lenses which determined the softness or hardness of ionization by variation of the degree of collisional activation in the medium-pressure regime,[13] two transfer octopoles, and a Paul ion-trap with ca. 10^{-3} mbar helium for ion storage and manipulation, including a variety of MS^n experiments.[14] For detection, the ions were ejected from the trap to an electron multiplier. Low-energy CID was performed by application of an excitation AC voltage to the end caps of the trap to induce collisions of the kinetically excited ions with the helium buffer gas. For a CID excitation period of 20 ms and a trapping parameter of $q_z = 0.25$, we have recently introduced an empirical calibration scheme that allows a conversion of the experimental collision energies to an absolute scale.[15]
[12] A. Tintaru, J. Roithová, D. Schröder, L. Charles, I. Jušinski, Z. Glasovac, M. Eckert-Maksić, *J. Phys. Chem. A* **2008**, *112*, 12097 – 12103.
[13] D. Schröder, T. Weiske, H. Schwarz, *Int. J. Mass Spectrom.* **2002**, *219*, 729 – 738.
[14] R. A. J. O'Hair, *Chem. Commun.* **2006**, 1469 – 1481.
[15] a) Á. Révész, P. Milko, J. Žabka, D. Schröder, J. Roithová, *J. Mass Spectrom.* **2010**, *45*, 1246 – 1252; b) E. L. Zins, C. Pepe, D. Schröder, *J. Mass Spectrom.* **2010**, *45*, 1253 – 1260.
[16] The general sequence for such hydroxylation reactions of alkanes by gaseous metal-oxide ions is: $R\text{-}H + MO^+ \rightarrow R\text{-}H/MO^+ \rightarrow R^{\bullet}/MOH^+$ or $R\text{-}MOH^+ \rightarrow R\text{-}OH/M^+ \rightarrow R\text{-}OH + M^+$; see Refs. [1] and [2].
[17] a) A. B. Kanu, P. Dwivedi, M. Tam, L. Matz, H. H. Hill, *J. Mass Spectrom.* **2008**, *43*, 1 – 22; b) B. C. Bohrer, S. I. Merenbloom, S. L. Koeniger, A. E. Hilderbrand, D. E. Clemmer, *Annu. Rev. Anal. Chem.* **2008**, *1*, 293 – 327; c) J. Puton, M. Nousiainen, M. Sillanpää, *Talanta* **2008**, *76*, 978 – 987.
[18] In brief, ion-mobility separation can be compared to chromatography in the condensed phase. An electric field gradient provides a driving force for the mobile phase, which consists of ions of interest. Collisional interactions with the inert gas (here N_2 at 2 mbar) serve as the stationary phase. Much like in electrophoresis, two isobaric ions of different shape ("potato and cigar"), the more compact one interacts less with the stationary phase and thus reaches the detector before the more extended (larger surface area) ion of identical mass.
[19] Ion-mobility mass spectrometry experiments were performed with a SYNAPT G2 ion-mobility mass spectrometer (Waters, Manchester, UK). For details on the experimental setup and its operation, see Refs. [17a] and [20].
[20] a) Á. Révész, D. Schröder, T. A. Rokob, M. Havlík, B. Dolenský, *Angew. Chem.* **2011**, *123*, 2449 – 2452; *Angew. Chem. Int. Ed.* **2011**, *50*, 2401 – 2404; b) D. Schröder, *Collect. Czech. Chem. Commun.* **2011**, *76*, 351 – 369.
[21] M. J. Frisch et al. Gaussian 09; Revision A.02, **2009**.
[22] For the method used to calculate the cross sections, see: Á. Révész, D. Schröder, T. A. Rokob, M. Havlík, B. Dolenský, *Phys. Chem. Chem. Phys.* **2012**, *14*, 6987 – 6995.
[23] See also: L. Jašíková, E. Hanikýřová, D. Schröder, J. Roithová, *J. Mass Spectrom.* **2012**, *47*, 460 – 465.
[24] For a review on gas-phase catalysis, see: D. K. Böhme, H. Schwarz, *Angew. Chem.* **2005**, *117*, 2388 – 2406; *Angew. Chem. Int. Ed.* **2005**, *44*, 2336 – 2354.

